The Pennsylvania State University
The Graduate School

THE USE OF LIGHT-INITIATED HYDROGEN ATOM TRANSFER TO MODIFY POLY(STYRENE), POLY(METHYLMETHACRYLATE), AND SQUALANE

A Thesis in
Chemistry
by
Daniel A. Knappenberger

Submitted in Partial Fulfillment
of the requirements
for the degree of
Master of Science

December 2023

The thesis of Daniel A. Knappenberger was reviewed and approved by the following:

Elizabeth Elacqua
Assistant Professor of Chemistry
Thesis Co-adviser

Robert J. Hickey
Associate Professor of Materials Science and Engineering
Thesis Co-adviser

Benjamin J. Lear
Professor of Chemistry

Eric D. Nacsa
Assistant Professor of Chemistry

Philip Bevilacqua
Distinguished Professor of Chemistry
Professor of Biochemistry and Molecular Biology
Head of the Department of Chemistry

ABSTRACT

Polyolefins are an important and ubiquitous class of commodity polymers in modern society. They possess remarkable stability and chemical resistance, making them highly desirable materials. These materials are often used as single-use plastics despite their biodegradability. Methods of recycling, such as mechanical recycling, post-polymerization modification (PPM), and depolymerization, can incentivize plastic waste collection by upcycling or adding value to the waste material. However, the lack of reactivity of polyolefins requires harsh conditions for PPM or depolymerization. Recent advances in C–H functionalization of both small molecules and polymers have allowed access to highly reactive intermediates under mild conditions, such as C-centered radicals at room temperature without the use of peroxides and heat. Unfortunately, functionalization above just a few mol% is accompanied by degradation of the polymer chain due to the highly reactive intermediates present. Therefore, new methods of PPM must be developed so that functionalization is preferred over polymer degradation. Alternatively, the degradation observed during PPM could be used to encourage polymer deconstruction.

In this thesis, three photocatalysts are investigated as potential catalysts to degrade polyolefins. The catalysts were chosen because of their reported ability to enable hydrogen atom transfer (HAT). Benzophenone (BP), tetrabutylammonium decatungstate (TBADT), and $FeCl_3$ are investigated with specific attention to squalane as a small molecule analog of poly(propylene) (PP). Spectroscopic analysis — ^{1}H NMR spectroscopy, ^{13}C APT NMR spectroscopy, IR spectroscopy, and APCI mass spectrometry — supports addition of BP to squalane to form an α-alkylbenzhydrol, while TBADT and $FeCl_3$ facilitated oxidation of squalane to alcohols and ketones. The results with BP support its tendency to form unintended C–C bonds with reactive intermediates, while the results with TBADT and $FeCl_3$ are consistent with their use as oxidation catalysts for hydrocarbons (*i.e.,* cyclohexane). These results may be used to show that BP could be attached to PP and that TBADT and $FeCl_3$ may be used to oxidize PP.

TABLE OF CONTENTS

LIST OF FIGURES

LIST OF ABBREVIATIONS

AP	Acetophenone
APCI	Atmospheric pressure chemical ionization
AQ	Anthraquinone
BDE	Bond dissociation energy
BP	Benzophenone
$CDCl_3$	Chloroform-*d*
DCBP	4,4'-dichlorobenzophenone
DCM	Dichloromethane
DIAD	Diisopropyl azodicarboxylate
DT	Decatungstate
Đ	Dispersity
GC	Gas chromatography
GPC	Gel permeation chromatography
HAT	Hydrogen atom transfer
HPLC	High performance liquid chromatography
ISC	Intersystem crossing
LMCT	Ligand–to–metal charge–transfer
MAH	Maleic anhydride
M_n	Number average molecular weight
NMR	Nuclear magnetic resonance
^{1}H NMR	^{1}H nuclear magnetic resonance

^{13}C APT NMR	^{13}C nuclear magnetic resonance with attached proton test
PBD	Poly(butadiene)
PE	Poly(ethylene)
PEG	Poly(ethylene glycol)
PMMA	Poly(methyl methacrylate)
PP	Poly(propylene)
PP-*g*-MAH	Maleic anhydride modified poly(propylene)
PPM	Post-polymerization modification
PS	Poly(styrene)
PVA	Poly(vinyl alcohol)
RAFT	Reversible addition fragmentation chain transfer
TBADT	Tetrabutylammonium decatungstate
TCE	1,1,2,2-tetrachloroethane
THF	Tetrahydrofuran
UV	Ultraviolet
XA	Xanthone

Chapter 1: Introduction

Commercial plastics are prevalent in modern life because they are cheap, lightweight, chemically inert, and durable.[1–3] Since 1950, the growth of global annual plastic production has outpaced all other manufactured materials.[4–6] However, many commercially available plastics accumulate in the environment because they are chemically inert. More than 6,300 million metric tons of plastic waste have been generated, almost 80% of which exists in landfills or as environmental pollution.[5,6] Poly(ethylene) (PE), poly(propylene) (PP), and poly(styrene) (PS) comprise more than 60% of global plastic production.[5] These materials are exceptionally durable and chemically inert because their backbones are composed of strong sp^3-hybridized C–C and C–H bonds (Figure 1).

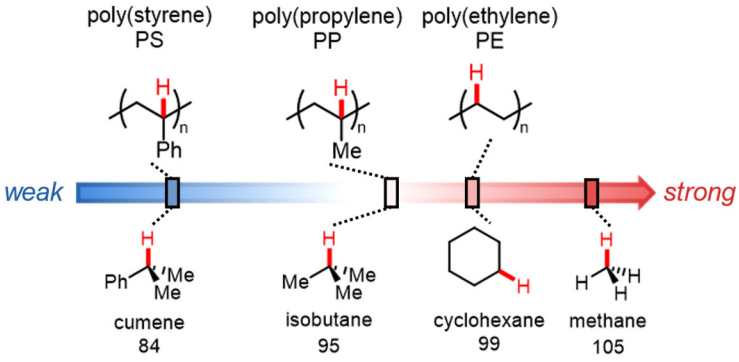

Figure 1: Bond dissociation energies of representative compounds of PS, PP, and PE.

This bond strength can be quantified in terms of bond dissociation energy (BDE): 84, 95, and 99 kcal/mol for cumene, isobutane, and cyclohexane, respectively.

Mechanical recycling is the most common method of recycling plastics. In this process, the plastic waste is separated, shredded, and processed in the melt phase. However, the separation process often leaves contaminants – other plastics, food residue, additives, *etc.* – that contribute to deleterious side reactions. Ultimately, the recycled material loses its original mechanical properties after just a few cycles.[5,7,8] Mechanical recycling, therefore, is referred to as "downcycling". It is essential to develop new strategies to chemically recycle plastic waste because downcycling offers little incentive to reclaim plastic waste.

Alternatively, plastic waste can be "upcycled" into new products. In this approach, plastic waste is reframed as a springboard to new polymers (diversification), small molecules (deconstruction), or high-performance materials.[1,9] Existing diversification methods suffer from poor selectivity because highly reactive species are required to activate strong sp^3 C–C and C–H bonds of polyolefins (Figure 2).[7] For example,

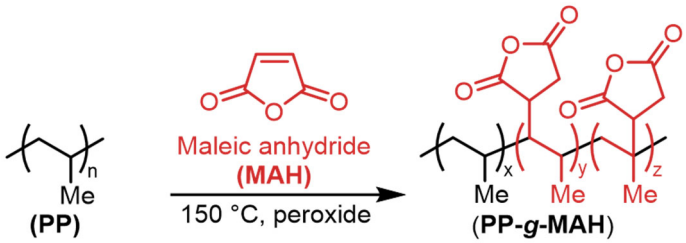

Figure 2: Typical industrial preparation of PP-*g*-MAH.

poly(propylene-graft-maleic anhydride) (PP-*g*-MAH) is commercially prepared through peroxide-initiated free radical PPM in the melt phase (>150 °C).[10] The combination of highly reactive intermediates and high temperatures decrease material uniformity because high temperatures promote *β*-scission. Ideally, the C-centered radicals react with maleic anhydride (MAH) to form a new C–C bond; however, this is not always the case. The C-centered radical of one chain of PP can react with the C-centered radical of another chain of PP to form "crosslinks" or promote "*β*-scission" — the spontaneous C–C cleavage of the bond *β*- to the radical (Figure 3). Scission is more likely to occur in polymers that can produce stabilized radicals (*e.g.*, PP, which can produce tertiary radicals).[11]

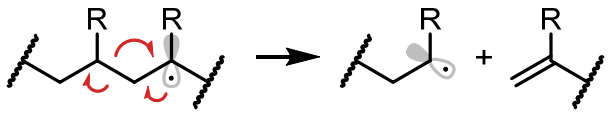

Figure 3: β-scission at a radical on a tertiary C, resulting in a new radical and C=C bond.

Polymers degrade predominately through *β*-scission at elevated temperatures.[12] The thermodynamics of polymerization are represented by the Gibbs free energy equation (Equation 1):

$$\Delta G_p = \Delta H_p - T\Delta S_p \quad (1)$$

Where ΔS_p and ΔH_p are the change in entropy and enthalpy during polymerization, respectively. It follows that there is a ceiling temperature, T_c, at which the rates of polymerization and depolymerization are equal, *i.e.* the concentration of monomer and polymer are in equilibrium[13] (Equation 2):

(2) $$T_c = \frac{\Delta H_p}{\Delta S_p}$$

At T_c, C–C bonds along the backbone spontaneously dissociate to generate terminal radicals on the backbone.[12] The radicals along the backbone can undergo further C–C cleavage through β-scission. However, there are processes below the ceiling temperature where C–C cleavage occurs through the generation of radicals along the polymer backbone. Oxidative degradation, sheer forces, and light are other methods of generating radicals along the backbone of polyolefins.[12,14,15] Other polymers with heteroatoms in the backbone, such as polyesters and polyurethanes, also degrade by glycolysis or hydrolysis in addition to β-scission.[16]

Pyrolysis is a method of deconstructing polymers through β-scission at elevated temperatures in the absence of O_2. Radicals are generated at random points along the polymer backbone, enabling cleavage of C–C bonds to yield short-chain hydrocarbons.[17,18] For example, Celik et al.[19] developed a $Pt/SrTiO_3$ catalyst that facilitates the pyrolysis of PE in the presence of H_2 at 300 °C. The number average molecular weight (M_n) was reduced from 64.3 kDa to 0.6 kDa. The reaction was successfully adapted to deconstruct a plastic bag; the M_n was reduced from 33.0 kDa to 1.0 kDa. In both cases, the products were a distribution of hydrocarbon oils. However, the chemical similarity of these products greatly complicates their isolation. Additionally, the catalytic system requires a precious metal (*e.g.*, Pt) to work effectively.

A major disadvantage to pyrolysis is the random nature of the polymer deconstruction, which generates many chemically similar products. A more precise process that generates a limited set of valuable products is highly desirable. Conk *et al.*[20] and Arroyave *et al.*[21] independently developed an alternative approach to deconstruct PE through dehydrogenation and metathesis/isomerization. First, dehydrogenation is used to install C=C bonds as reactive handles along the backbone. Then, the metathesis catalyst and ethylene break the C–C bond adjacent to the C=C bond, generating a terminal alkene and propene. The isomerization catalyst converts the terminal alkene into an internal alkene. Finally, the metathesis catalyst and ethylene convert the internal alkene into

propene. Although the process produces a valuable feedstock — propene — it requires precious metals (Ir, Ru, and Pd) and ethylene at high pressures.

Thermally driven methods of polymer deconstruction generate many products because radicals are generated at random points along the backbone of the polymer; therefore, a controlled method of generating radicals along the backbone of the polymer would reduce the number of products generated. Hydrogen atom transfer (HAT) processes are used to activate the relatively inert C–H bonds of small molecules and polymers (Figure 4).[1] Similar to reactions of polyolefins, the small molecule reactions traditionally require toxic or harsh reagents for activation, such as tributyltin[22] or peroxides and high temperatures[23]. Fortunately, recent advances in synthetic organic chemistry have resulted in processes that use light to generate highly reactive intermediates that activate C–H bonds under mild conditions.[23]

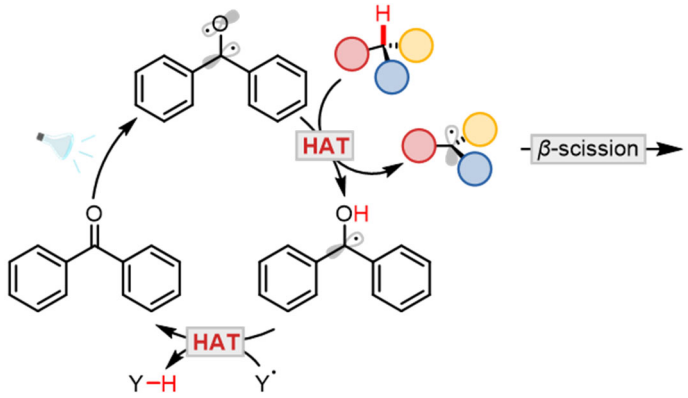

Figure 4: General photocatalytic HAT scheme with BP as the photocatalyst. PC = photocatalyst, Y = H-atom acceptor

Fazekas *et al.*[24] developed a process which modifies the C–H bonds of PE and PP through HAT. The major side reaction that occurs during PPM — *β*-scission — is a result of the production of radicals on tertiary C-atoms, which have a relatively long lifetime compared to radicals on secondary- or primary C-atoms. Thus, the authors chose a highly reactive, sterically hindered radical trap to prevent *β*-scission. Although the authors produced functionalized PE that had properties markedly different from the parent material, they were only able to achieve less than 4% functionalization without *β*-scission. This is an improvement to previous works that achieved 1–2% functionalization,[25,26] but these yields remain much lower than those observed for small molecules, where the substrate can be used as the solvent.[23]

Alternatively, HAT could be used to generate C-centered radicals on the backbone as "weak points" to promote C–C bond cleavage. If tertiary C-atoms are targeted, the generation of radicals could promote *β*-scission. Oh *et al*.[27] and Li *et al*.[28] used ferric chloride and fluorenone, respectively, to deconstruct PS into benzoic acid, benzaldehyde, and other aromatic products that can be used as chemical feedstocks. Additionally, Kong *et al.*[29] used TBADT and DIAD to deconstruct PE into functionalized oligomers. We were inspired by these works to apply HAT deconstruction to other polymers, such as PP. We envisioned that this approach would trigger deconstruction of PP due to the formation of radicals on tertiary C-atoms.

For PPM methods, there is a delicate balance between desired C–H functionalization and undesirable side reactions that result in polymer degradation.[1] It is also established that PP degradation pathways primarily follow a HAT mechanism: following macroradical generation, cleavage of C–C bonds is caused by *β*-scission.[30] The occurrence of *β*-scission is indicated by formation of *π*-bonds (C=C or C=O in oxidative mechanisms), a decrease in M_n, and an increase in $Đ$.

Thesis overview

Different H-atom abstractors were investigated for their ability to alter squalane, poly(styrene), and poly(methyl methacrylate) to induce *β*-scission. Squalane was used as a small molecule analog of poly(propylene) to narrow the variety of products that may be generated through deconstruction. Chapter 2 focuses on the ability of benzophenone to abstract H-atoms from poly(styrene), poly(methyl methacrylate), and squalane. Chapter 3 introduces other HAT catalysts: tetrabutylammonium decatungstate and ferric chloride as H-atom abstractors for squalane. Finally, concluding remarks are discussed in Chapter 4.

Chapter 2: Hydrogen atom transfer from poly(methyl methacrylate), poly(styrene), and squalane to benzophenone for C–H functionalization

2.1: Background

Aromatic ketones, such as benzophenone (BP), are well-known for their reactivity when excited by near-UV light.[23] When excited by light, an electron is promoted to the singlet state, then undergoes intersystem crossing (ISC) to a triplet state, BP*, that is similar in reactivity to an alkoxy radical.[23] The O-centered radical abstracts an H-atom from the substrate, R–H, to generate another radical, R$^{\bullet}$, and a reduced species, BP–H. Then, BP is restored through hydrogen atom transfer (HAT) to another substrate. Aromatic ketones are soluble in the nonpolar solvents required to dissolve polymers and are relatively cheap and commercially available. Irradiation of poly(styrene) (PS), poly (methyl methacrylate) (PMMA), and squalane in the presence of BP will result in the generation of C-centered radicals. These radicals can incite β-scission or couple with each other (Figure 5).

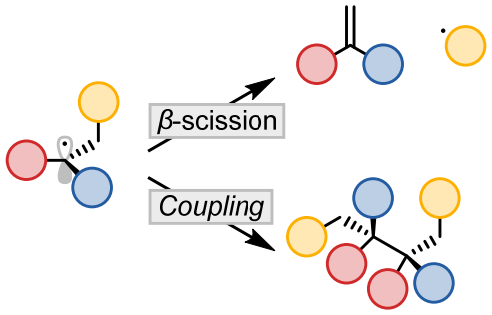

Figure 5: Depiction of the fate of the C-centered radical: *β*-scission (top) or coupling with another C-centered radical (bottom).

2.2: Poly(methyl methacrylate) and poly(styrene)

BP was first investigated as an initiator of deconstruction of PMMA and PS. PMMA lacks a tertiary C-atom, which should preclude its potential for deconstruction. On the other hand, PS should be more prone to deconstruction because HAT from the tertiary C-atom will generate a stabilized benzylic radical. Gel permeation chromatography (GPC) was used as the main characterization technique because deconstruction should result in a decrease in number average molecular weight (M_n). An increase in M_n suggests that radical termination occurred between polymer chains. Both PS (M_n = 31.9 kDa and $Đ$ = 1.03; from anionic polymerization) and PMMA (M_n = 14.9 kDa and $Đ$ = 1.49; from free-radical

polymerization) were irradiated with varied concentrations of BP (mol%), with respect to moles of polymer chains, at 370 nm. PMMA reactions were run in acetonitrile, while PS reactions were run in dichloromethane (DCM) due to better solubility.

Irradiation of PS resulted in a decrease in M_n and an increase in dispersity ($Đ$) (Figure 6). indicating that degradation occurred in the presence (M_n = 27.2 kDa, $Đ$ = 1.27)

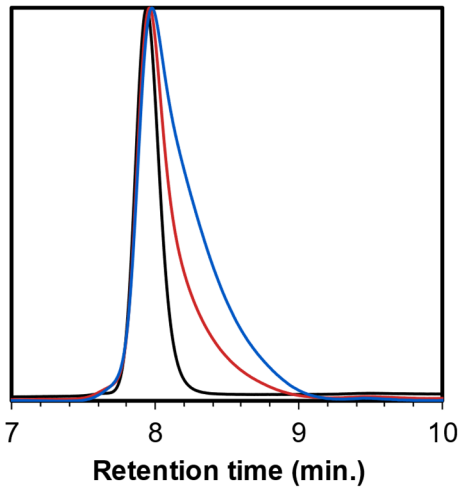

Figure 6: GPC trace of PS (black), PS at 370 nm (blue), PS with 1 mol% BP at 370 nm (red). Refractive index detector used.

and absence (M_n = 17.1 kDa, $Đ$ = 1.38) of BP. It is known that exposure to light with $\lambda <$ 400 nm promotes PS degradation in the presence[31] or absence of BP.[32] Mita et al. observed that BP promoted degradation of PS; however, we observed that the presence of BP slowed degradation. It is possible that low amounts of BP act like a "sunscreen" for PS: the UV light is absorbed by BP instead of PS, and HAT does not occur from the backbone of PS.

Irradiation of PMMA (M_n = 13.3 kDa, $Đ$ = 1.50) in the presence of BP (*vide supra*) resulted in a slight increase in UV absorbance by GPC (Figure 7). This is significant

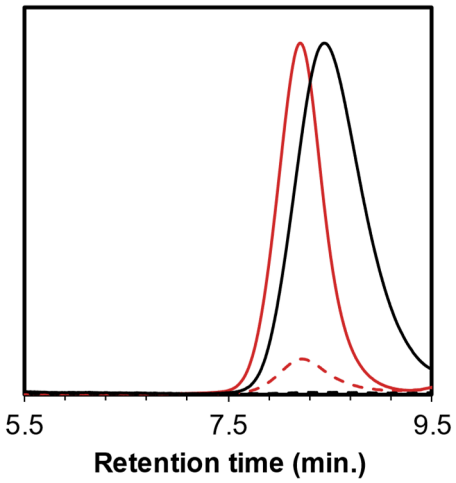

Figure 7: GPC traces of PMMA (black) and PMMA with 1 mol% BP at 370 nm (red). Solid lines are the refractive index detector trace and dotted lines are the UV detector trace.

because unmodified PMMA is nearly undetectable on the UV detector trace. PMMA synthesized by RAFT (M_n = 23.8 kDa and $Đ$ = 1.09) was irradiated at 390 nm in the presence of BP (M_n = 54.3 kDa and $Đ$ = 1.04) (Figure 8). Interestingly, the M_n of PMMA approximately doubled following irradiation in the presence of BP. It is possible that

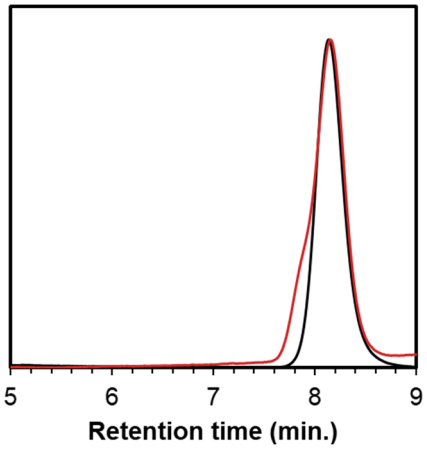

Figure 8: GPC traces of RAFT-synthesized PMMA (black) and RAFT-synthesized PMMA with 1 mol% BP at 370 nm (red). Refractive index detector used.

exposure to UV light caused dissociation of the thiocarbonylthio chain end (Figure 9) to yield a PMMA macroradical.[33] Then, the macroradicals terminated together, doubling the M_n of the polymer.

The large size of the polymer chains of PS and PMMA precluded investigation of the location of C–C cleavage or functionalization by BP. A small molecule model system was selected to enable more facile investigation of the BP system.

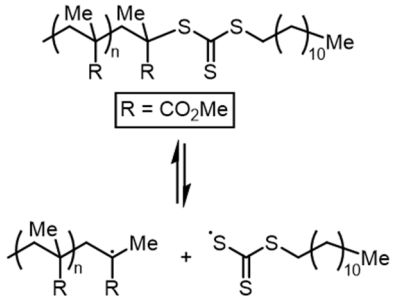

Figure 9: Dissociation of the thiocarbonylthio end group from PMMA.

2.3: Squalane

A small molecule system was chosen to better elucidate the degradation products. Squalane was chosen as a small molecule because it is commercially available and possesses six tertiary C-atoms, which likely have similar C–H BDEs to PP (Figure 10). As

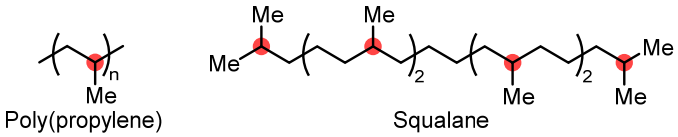

Figure 10: Structures of PP and squalane. Tertiary C-atoms are highlighted in red.

previously mentioned, PP should be prone to β-scission because of its tendency to form tertiary radicals. Regularly placed methyl groups along the backbone may also produce a steric environment like that in PP. PS tends to degrade in near-UV light, while PMMA does not possess tertiary C-atoms. Therefore, PP was chosen as the target polymer system.

To mimic the conditions that would be used for the polymeric system, one equivalent of BP for each tertiary C–H bond – corresponding to six equivalents of BP for each molecule of squalane – was used (Figure 11). Irradiation of squalane in the presence

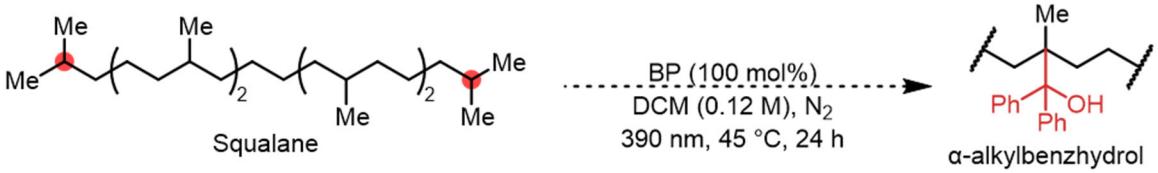

Figure 11: Conditions for squalane/BP reactions.

of BP yielded an amber oil. The crude product mixture was triturated with cold *n*-hexanes to separate the oil from BP.

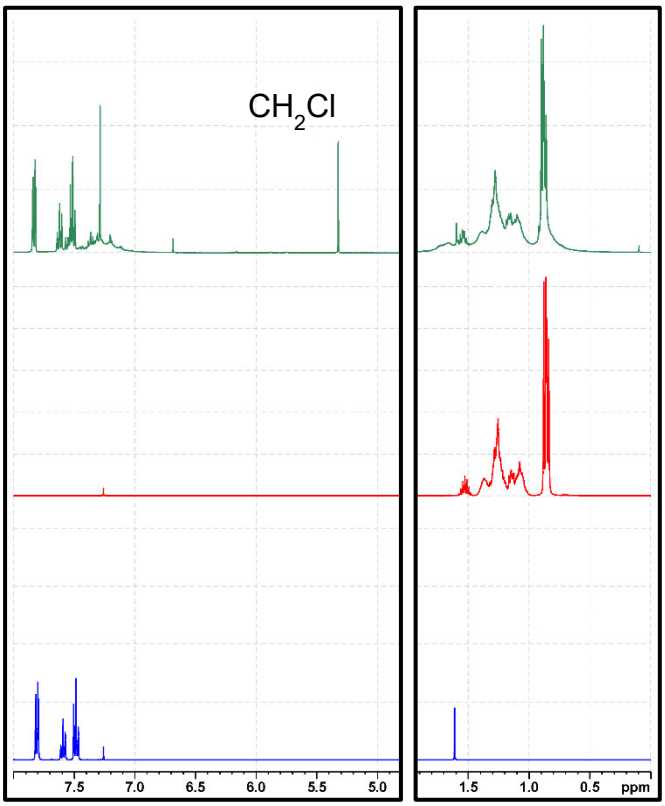

Figure 12: ^{1}H NMR spectra of BP (blue), squalane (red), and the triturated product (green) in $CDCl_3$.

NMR spectroscopy was used to analyze the product to gain broad insight into the structural nature of the products. The ^{1}H NMR spectrum of the extracted oil in $CDCl_3$ featured peaks shifted downfield relative to squalane, upfield relative to BP, and a peak at 3.5 ppm (Figure 12). Peaks associated with the vinylic protons (5–6 ppm) expected of C=C

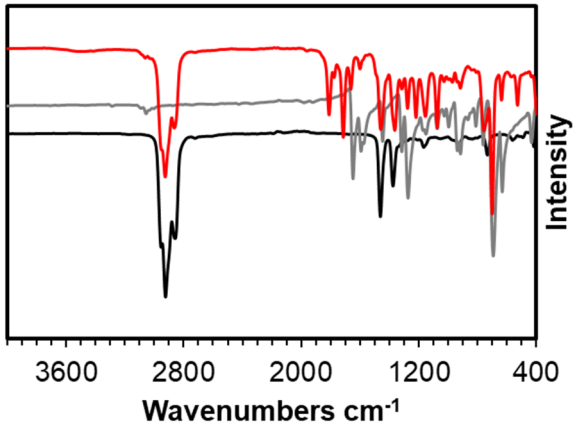

Figure 13: IR spectra of squalane (black), BP (gray), and the product (red).

bond formation were absent, indicating that β-scission did not occur. The location of the observed aliphatic and aromatic peaks is consistent with reported ^{1}H NMR spectra of α-alkylbenzhydrols of paraffin and BP.[34] The ^{13}C APT NMR spectra feature a new positive peak — corresponding to a tertiary or primary carbon — in the aliphatic region (32 ppm) (**Figure 24**). Formation of an α-alkylbenzhydrol should be accompanied by an –OH group. Although the –OH group can be detected by NMR spectroscopy, it was not observed because the hydrogen bonding reduces the reliability of detection.

The IR spectrum of the product (Figure 13) featured a faint broad peak in the region of 3600–3300 cm^{-1}, and peaks in the region of 1800–1700 cm^{-1}, corresponding to O–H and C=O stretching, respectively. The former is expected of α-alkylbenzhydrol formation (Figure 14); however, the latter is unexpected, because there is only one peak in the ^{13}C

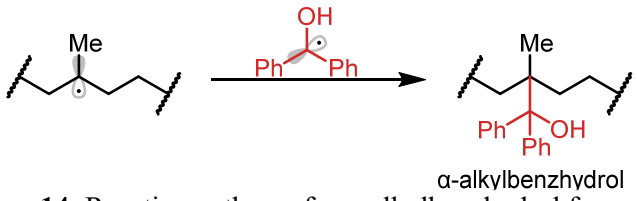

Figure 14: Reaction pathway for α-alkylbenzhydrol formation.

APT NMR spectra — at 196 ppm — which corresponds to the carbonyl carbon of remaining BP. The other carbonyl stretches in the IR spectrum are unaccounted for in the ^{13}C APT NMR spectrum. The stretch at 1805 cm^{-1} is consistent with an acid halide or acid anhydride, while the stretch at 1710 cm^{-1} is consistent with a ketone or aliphatic carboxylic acid. These peaks are unattributed to BP, as its C=O stretch is located around 1650 cm^{-1}. BP is known to possess long-lived reactivity after irradiation,[34] which may be responsible for producing oxidized species.

Finally, the samples were analyzed by atmospheric pressure chemical ionization mass spectrometry (APCI–MS) to determine whether there were multiple BP molecules attached to the squalane molecules. The most prominent peak associated with the product is at m/z = 603.5 in the positive ion spectrum; however, this value is inconsistent with the

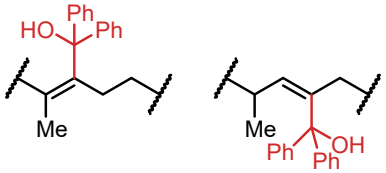

Figure 15: Examples of α-alkylbenzhydrol products featuring a π-bond.

expected m/z of the α-alkylbenzhydrol (m/z = 605.6) and indicates an additional unit of unsaturation (a ring or π-bond) present in the structure (Figure 15).

2.4: Conclusion

The observed spectra are consistent with a change to the chemical environment of squalane. However, the spectra are inconsistent with each other. The ^{1}H NMR displayed no evidence of vinylic H atoms, which are indicative of C=C bond formation. The ^{13}C APT NMR spectrum contained only C=O signals associated with BP. Additionally, any signals that would indicate C=C bond formation in squalane were obscured by signals associated with aromatic C=C bonds. However, the APCI–MS had a prominent peak at m/z = 603.5, indicating π-bond formation. Observed ^{1}H NMR spectra are consistent with reported spectra of α-alkylbenzhydrols of paraffin and BP; a small amount of O–H stretching is present in the IR spectra; and APT NMR spectra contain new aliphatic peaks associated with tertiary or primary substituted carbon atoms. However, further details remain elusive: the location of C–C bond formation and the nature of the carbonyl products observed by IR spectroscopy. Additionally, BP has undesirable reactivity in its reduced state, resulting in C–C bond *formation*. Ultimately, BP does not support the goal of triggering C–C bond cleavage; therefore, an alternative HAT initiator was selected. Future work may focus on choosing an aromatic ketone that does not have the tendency to form C–C bonds. Known compounds such as anthraquinone could be investigated, or a derivative of BP with a sterically hindered C=O bond could be synthesized. However, we chose to avoid this issue altogether by choosing H-atom abstractors that would not form C–C bonds with squalane: TBADT and $FeCl_3$.

Chapter 3: Hydrogen atom transfer from squalane to inorganic hydrogen-atom abstractors for C–H functionalization

3.1: Background

The primary issues encountered with BP were related to separation and purification of the product(s) (*i.e.*, BP could not be fully separated from reacted squalane) and C–C bond formation. Inorganic H-atom abstractors — DT and $FeCl_3$ — were chosen to remedy the issues encountered with BP. The mechanism of DT is like BP: excitation by light triggers a transfer of electrons away from the oxygen atoms. The highly electronegative oxygen atoms, like the oxygen atom of BP, abstract H atoms from aliphatic C–H bonds.[35] DT is reported to break strong C–H bonds, such as those in methane (BDE = 105 kcal/mol).[23,36] A strong H-atom abstractor such as DT may facilitate more HAT from squalane and cause more β-scission.

On the other hand, $FeCl_3$ operates by LMCT. Excitation by light triggers homolytic cleavage of the Fe–Cl bond to generate $Cl^{\bullet}$ and Fe^{II}.[27] Then, $Cl^{\bullet}$ abstracts an H atom from the substrate to generate HCl (BDE = 103 kcal/mol).[37] This bond is also stronger than the C–H bond of a tertiary carbon (BDE = 95 kcal/mol).[37] $FeCl_3$ is known to abstract H atoms from aliphatic hydrocarbons, such as 2-methylpentane.[38] Oh and Stache[27] recently reported that $FeCl_3$ and light leads to the formation of radicals on the backbone of PS, promoting deconstruction.

3.2: Decatungstate for hydrogen atom transfer

The DT anion, $[W_{10}O_{32}]^{4-}$, is a polyoxometalate with well-reported photochemical reactivity.[23,36,39–41] For example, photoexcited DT has been documented to abstract hydrogen atoms from very strong C–H bonds, including methane (BDE = 105 kcal/mol). DT is effective at low catalyst loadings because it does not dimerize like aromatic ketones.[23,35] Noting the impressive reactivity of TBADT, we were inspired to investigate DT as an initiator for the deconstruction of squalane. TBADT was synthesized according to a literature procedure[42] and the UV-visible absorbance spectrum and cyclic voltammogram were consistent with previous reports.[43,44] The tetrabutylammonium salt

was used because it is more soluble in organic solvents than the sodium salt.[23,45] The C–H functionalization of THF with DIAD was successfully replicated from a literature procedure,[46] supporting that TBADT could initiate HAT within the experimental design.

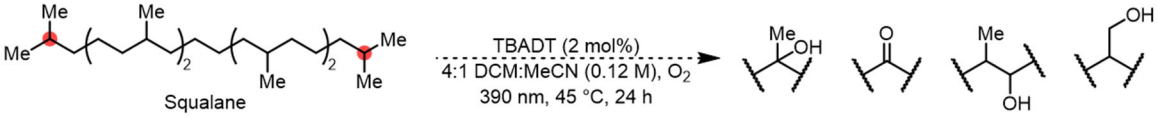

Figure 16: Scheme for reactions between squalane and TBADT.

Irradiation of squalane in the presence of TBADT (Figure 16) resulted in a deep blue solution, often accompanied by a blue precipitate. The UV-visible absorbance spectrum (Figure 17) of the irradiated product was recorded immediately after the vessel

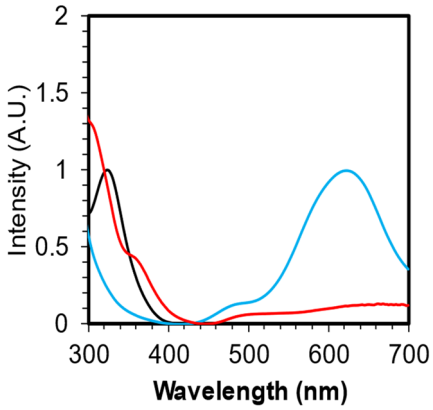

Figure 17: UV-Visible spectra of TBADT (black), TBADT after 5 minutes of irradiation (λ = 390) (blue), and the reaction mixture after 24h of irradiation (red).

was removed from the light. Several irradiated solutions featured an absorption at λ = 370 nm, consistent with the monoreduced $H^+[W_{10}O_{32}]^{4-}$ species that forms as a result of HAT.[47] The solvent was removed from the product mixture prior to qualitative characterization by ^{1}H NMR spectroscopy.

A distinct feature of the ^{1}H NMR spectrum of squalane (Figure 18) is the nonet at 1.55 ppm, which is associated with the terminal tertiary protons of squalane (Figure 16). Changes to the multiplicity and relative intensity of this signal suggest alteration in the chemical environment of these protons. Functionalization of adjacent C–H bonds would result in a decrease of the nonet multiplicity because the H atoms responsible for the nonet

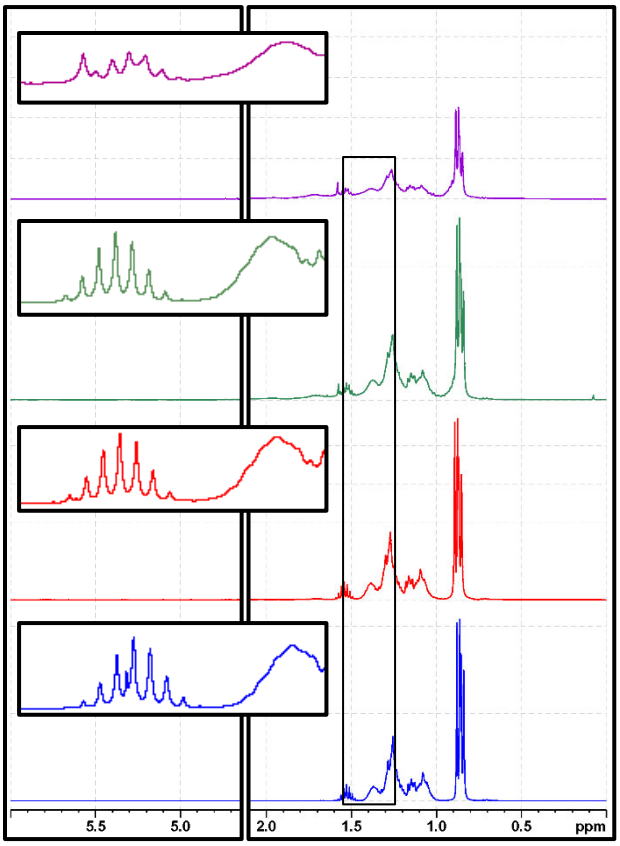

Figure 18: ^{1}H NMR spectra of squalane (blue), reaction in N_2 (red), reaction with O_2 and dry solvent (green), and reaction with O_2 and solvent used as-is (purple).

are diminishing. Alternatively, functionalization of the tertiary C-atoms would result in a decrease in the nonet intensity because functionalization would cause the tertiary C-atoms to become quaternary. Although this does not provide information about the entire molecule, it can be used as a snapshot of the structure. The multiplicity of the nonet changes only in the presence of O_2 and as-is solvent. The nonet centered around 1.55 ppm — corresponding to the two terminal tertiary protons — of reacted samples was compared to that of the starting material. The most notable features of the product mixture are a broad multiplet centered around 1.71 ppm — downfield of the original peak — and suppression of the nonet. The changes were most noticeable upon irradiation of squalane in the presence of O_2 (or constant stream of air) and solvents containing water (*i.e.,* used as-is without drying). Solvents containing water were used because the water molecules may be used as a source of hydroxyl radicals, triggering further oxidation. Crude products with ^{1}H NMR spectra markedly different from the starting material (*i.e.,* exhibited a change to the nonet

at 1.71 ppm, meaning that a notable change in chemical environment occurred) were further analyzed by IR spectroscopy and APCI–MS.

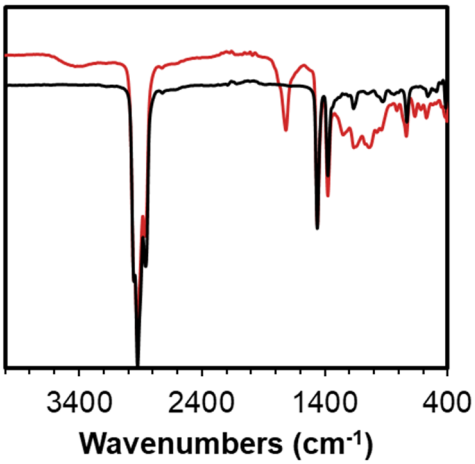

Figure 19: IR spectra of squalane (black) and oxidized sample (red).

Products such as alcohols, ketones, aldehydes, and carboxylic acids are expected from an oxidative mechanism. These functional groups have distinct peaks in IR spectra. The IR spectra of the mixtures (Figure 19) feature two new peaks at 3300–3600 (broad) and 1718 cm^{-1}, corresponding to O–H stretching and C=O stretching, respectively. Although the O–H stretch may be attributed to absorbed water, the C=O stretch can only come from the product. The presence of C=O stretching indicates that the reaction conditions facilitated oxidation of squalane. However, it is unclear whether oxidation of a secondary C-atom or oxidation and β-scission occurred. Oxidative degradation of polyolefins proceeds through a free radical mechanism accompanied by β-scission, resulting in products with carboxylic acid, ketone, aldehyde, and hydroperoxyl functional groups.[48] Carbonyl-containing functional groups result from β-scission of the C–C bond α-to the alkoxy radical or oxidation at a secondary carbon atom.

Squalane was irradiated in the presence of TBADT and DIAD (radical trap). Ethylene carbonate was added as an internal standard to quantify the amount of reacted DIAD. The ^{1}H NMR spectrum of the DIAD-functionalized squalane features a septet around 5.0 ppm, which is upfield relative to the septet of DIAD, consistent with addition of DIAD to an aliphatic substrate (Figure 25). The evidence supports the oxidation of squalane initiated by TBADT. Reactions in the presence of air and water resulted in more changes to the ^{1}H NMR spectra of the products. The IR spectra of the products also featured

O–H and C=O stretching, consistent with oxidation products. This led us to hypothesize that *deconstruction of squalane could be driven by a HAT-oxidation mechanism* (Figure 20). First, radicals are generated on the backbone (through HAT, heat, or light) and O_2

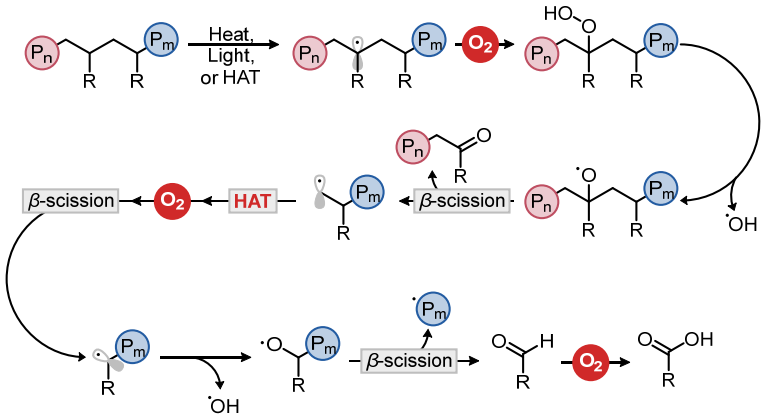

Figure 20: Mechanism of oxidative degradation of polyolefins.

from the atmosphere reacts to generate a hydroperoxide species. The O–O bond breaks, leaving an alkoxy radical, which undergoes *β*-scission, generating a ketone and a primary radical. Through repeated HAT, oxidation, and *β*-scission, further fragmentation occurs to form aldehydes and carboxylic acids. This is valuable information; however, it turned out that the impressive reactivity of TBADT was insufficient for deconstruction of squalane because its solubility contrasts with that of squalane. This was demonstrated by the blue precipitate that was frequently present in the product mixtures. The presence of the precipitate possibly represents TBADT "stuck" in a catalytic cycle, where it cannot turn over and initiate more HAT oxidation of squalane. Despite the impressive reactivity of DT, its selectivity is dominated by steric hinderance.[41] Thus, the desired target — the C–H bonds of tertiary C-atoms[49] — was at odds with the selectivity of DT. These factors of solubility and selectivity led to the selection of a new photocatalyst.

3.3: Ferric chloride for hydrogen atom transfer

$FeCl_3$ is well-reported to promote photooxidative degradation of polyolefins,[27,38,50] and has gained attention as a photocatalyst in synthetic methodology involving small

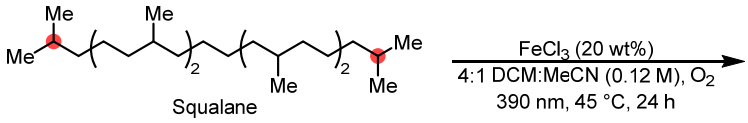

Figure 21: Conditions for squalane and $FeCl_3$ reactions.

organic molecules.[51] UV or visible light triggers homolysis of the Fe–Cl bond, generating Cl•. Therefore, $FeCl_3$ could be considered as a source of highly reactive Cl-radicals. Recent works[27,28,52,53] have reported that treatment of PS with $FeCl_3$ as a HAT initiator results in deconstruction, primarily yielding benzoic acid accompanied by a marked decrease in M_n. The Cl-radicals abstracted H-atoms from the tertiary C-atoms of PS, resulting in a macroradical, which ultimately led to continued β-scission. Again, squalane was used as a small molecule model of PP.

In the mechanism, Cl• abstracts an H atom from the polymer to generate a macroradical, which is critical for the oxidative degradation of polyolefins (Figure 20).The macroradical reacts with O_2 (from air) to generate a peroxyl radical (ROO•). The peroxyl radical abstracts another H atom to generate a hydroperoxyl species (RO–OH), which has a weak O–O bond that readily homolyzes to yield an alkoxy (RO•) and hydroxyl (HO•) radical. The alkoxy radical undergoes β-scission to generate two polymer chains: one with a terminal ketone, and the other with a terminal primary carbon radical. This mechanism propagates until small molecule products are generated. Additionally, this oxidative

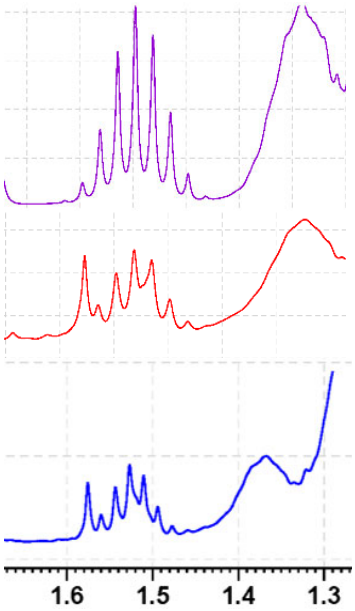

Figure 22: ^{1}H NMR spectra of squalane (purple), reaction of squalane and TBADT in O_2 (red), and reaction of squalane and $FeCl_3$ in air (blue).

degradation mechanism is largely understood to be the primary mode of degradation for other polyolefins such as PE and PP.[14,50]

Inspired by observations with TBADT and recent work with $FeCl_3$, reactions of squalane and $FeCl_3$ were investigated (Figure 21). Squalane and FeCl3 were dissolved in a mixture of 4:1 DCM:MeCN and irradiated for 24 hours at 390 nm. The product was characterized by ^1H NMR spectroscopy (Figure 22). The ^1H NMR spectrum of squalane irradiated in the presence of $FeCl_3$ and air appeared to be like that of the reactions between squalane and TBADT. The nonet decreased in intensity and there was a new multiplet downfield relative to squalane. This suggests that the $FeCl_3$ system required less O_2 to proceed, suggesting that $FeCl_3$ was a more potent photocatalyst than DT.

The IR spectrum (Figure 23) contains strong peaks at 1800 and 1770 cm^{-1}, 1160 cm^{-1}, and 1070 cm^{-1}, and a broad peak centered around 3400 cm^{-1}. These features indicate

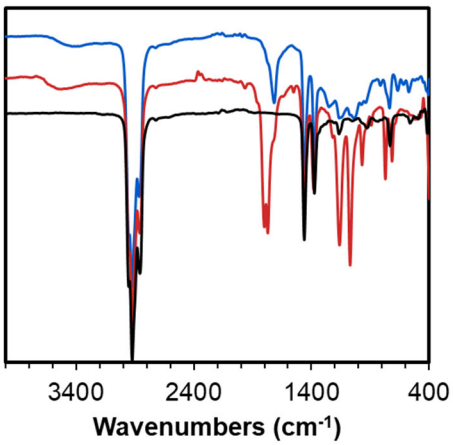

Figure 23: IR spectra of squalane (black), reaction of squalane and TBADT in O_2 (blue), and reaction of squalane and $FeCl_3$ in air (red).

C=O stretches, a secondary alcohol C–O stretch, a primary alcohol C–O stretch, and an O–H stretch, respectively. The location of the C=O peaks of the $FeCl_3$ reaction differs from that of the TBADT reaction. These C=O peaks are likely from ethylene carbonate — added as an internal standard for ^1H NMR — which has C=O peaks at 1800 and 1770 cm^{-1}. Although the chemical shift of the C=O peaks suggest an acid anhydride, it is unlikely that acid anhydrides were present because they typically decompose into carboxylic acids in the presence of water.[54] Surprisingly, there were no tertiary alcohol C–O stretches (1210–1100 cm^{-1}), which would be expected if HAT from a tertiary C-atom occurred. The IR spectrum suggests that HAT occurred from primary and secondary C-atoms.

3.4: Conclusion

The C–H oxidation of squalane was observed for both catalysts — TBADT and $FeCl_3$. Both reacted samples of squalane contained IR signals consistent with C=O bonds. Based on work by Oh and Stache,[27] carboxylic acids should be produced by oxidative deconstruction of squalane. The 1H NMR spectra contain significant changes to the nonet centered at $\delta = 1.55$ ppm, indicating that the chemical environment around protons of the terminal tertiary C-atoms (Figure 21) changed. Small amounts of O–H stretching were observed in both cases, but it is unclear whether this is from the reacted material or from absorbed water.

Chapter 4: Concluding remarks

Plastics possess highly desirable properties; however, these same properties cause them to accumulate in the environment. The work described herein focused on adapting small molecule methodology — photocatalytic HAT — to deconstruct polymers. Initially, PS and PMMA were targets of deconstruction; however, the plethora of potential degraded products precluded more detailed chemical analysis. Eventually, squalane was chosen as a model system for PP because it is a small molecule analog that was predicted to elucidate mechanistic pathways not easily detectable in macromolecules (*i.e.*, polymers). Three photocatalysts — BP, TBADT, and $FeCl_3$ — were used. However, the choice of squalane precluded facile analysis of the system. It was found that BP reacted with squalane to form a C–C bond, along with one unit of unsaturation (confirmed by APCI-MS). Next, TBADT oxidized squalane, as evidenced by the presence of C=O stretching by IR spectroscopy and the nature of the reaction conditions (in air, non-dried solvent). Finally, $FeCl_3$ was also found to oxidize squalane, as evidenced by the presence of C=O stretching by IR spectroscopy.

As a direct follow-up to this work, deconstruction of PP should be investigated with the aforementioned catalytic systems. A major challenge to this future work is that PP does not have the same solubility as squalane, so reactions must be run at elevated temperatures (> 100 °C). It is known that β-scission is more likely to occur at elevated temperatures.[12] Kong et al. investigated the deconstruction of PE in the presence of DIAD, noting that TCE solubilized both TBADT and PE.[29] To mitigate issues with solubility, initial studies could use atactic PP. A successful deconstruction reaction would yield quantifiable small molecule products, similar to the work done by Oh and Stache with PS.[27] Further studies could expand to include isotactic PP, which is commonly found in consumer-grade PP. Finally, the effect of additives commonly present in PP could be studied, by adding the additives individually and evaluating the obtained product distribution.

Other future work may focus on changing the polymer or catalyst. The choice of a polymer and catalyst that are soluble in the same non-halogenated solvent is ideal because halogenated solvents are environmentally hazardous. The ideal ‘green’ solvent is water; however, commodity plastics are insoluble in water. A possible future direction is to grind

the polymer into fine powder — to maximize surface area — and disperse it in an aqueous solution of photocatalyst. This would work for inorganic photocatalysts DT and $FeCl_3$.

Additionally, a polymer with C–H BDE lower than PP, such as PBD (allylic C–H BDE = 82 kcal/mol)[37] or PVA (RCH(OH)R' BDE = 91 kcal/mol) should be investigated — a lower BDE decreases the barrier to HAT and enables more facile evaluation of whether repeated HAT will promote *β*-scission. Another approach to lower the C–H BDE is to add electron-withdrawing atoms, such as N or O, *α*- to the C–H bond that is desired to be broken, such as PVA or PEG.

Other photocatalysts may be evaluated for deconstruction of polymers. Previous reports indicate that *β*-scission is more likely to occur when stabilized radicals (*e.g.*, a radical on a tertiary vs. a secondary C-atom) are formed.[12,49] Small H-atom abstractors should be selected to target tertiary radical formation. The chlorine radical, $Cl^{\bullet}$, shows some promise because it is highly reactive compared to the C–H bond (H–Cl BDE = 103 kcal/mol, isobutane C–H BDE = 95 kcal/mol)[37] and is not sterically hindered like BP or TBADT.

APPENDIX

Chemical spectra

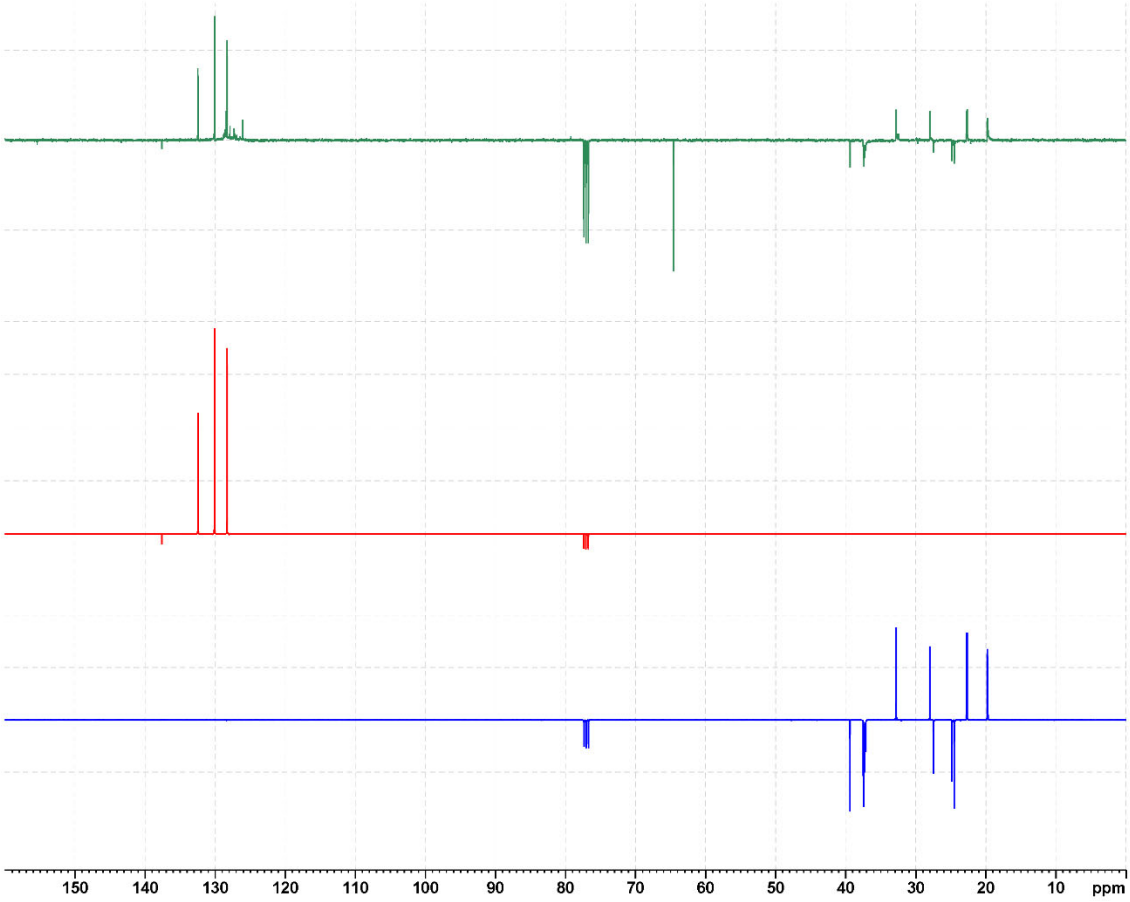

Figure 24: ^{13}C APT NMR spectra of squalane (blue), BP (red), and triturated product (green).

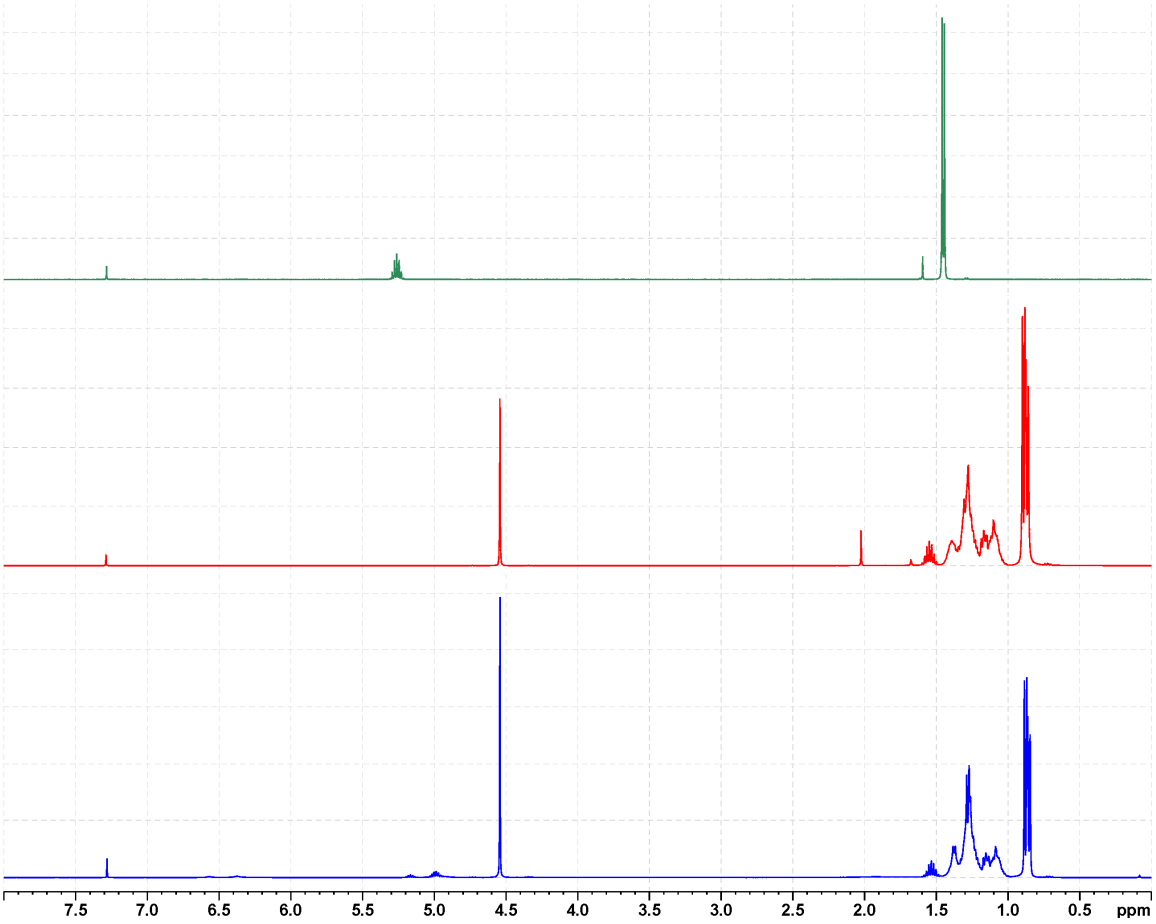

Figure 25: ^{1}H NMR spectra of squalane-DIAD (blue), squalane (red), and DIAD (green).

General reagent information

All reagents were purchased from Sigma Aldrich, Oakwood Chemical, Acros, Beantown Chemical, Tokyo Chemical Industry America, or Thermo Fisher Scientific. NMR spectra were collected on a Bruker Avance 400 MHz spectrometer using $CDCl_3$ as a solvent, unless otherwise indicated. UV-Visible absorption spectra were collected on an Agilent Cary 60 UVvisible spectrophotometer (Agilent Technologies, Inc.) using a quartz cuvette (Starna Cells). IR transmittance spectra were collected on a Nicolet iS10 with a Smart iTX ATR attachment (Shimadzu). Samples were prepared for GPC by dissolving the sample and filtering the solution through a 0.45 µm filter. GPC traces were collected on a Tosoh EcoSEC equipped with both Refractive Index (RI) and Ultraviolet (UV) detectors. Number average molecular weights (M_n) and weight average molecular weights (M_w) were calculated relative to linear poly(methyl methacrylate) standards.

Air-free photochemical reaction conditions – poly(methyl methacrylate)

To a 1 dram vial with a septum cap, poly(methyl methacrylate) (50 mg, M_n = 12.88, Đ = 1.49) and benzophenone were dissolved in acetonitrile (2.3 mL) with sonication. A 0.7 cm stir bar was added and the vial was sealed. The solution was purged with N_2 for 15 minutes. The vial was placed on a stir plate, 2 cm away from a Kessil 390 nm lamp and irradiated for 24 h. A fan was used to keep the temperature low. The solvent was removed, and the sample was redissolved in 0.7 mL CDCl3 for NMR spectroscopy. Approximately 2-4 mg of sample were dissolved in tetrahydrofuran (THF) for GPC.

Air-free photochemical reaction conditions – poly(styrene)

To a 1 dram vial with a septum cap, poly(styrene) (50 mg, M_n = 31.86, Đ = 1.03) and benzophenone were dissolved in dichloromethane (2.3 mL) with sonication. A 0.7 cm stir bar was added and the vial was sealed. The solution was purged with N_2 for 15 minutes. The vial was placed on a stir plate, 2 cm away from a Kessil 390 nm lamp and irradiated for 24 h. A fan was used to keep the temperature low. The solvent was removed, and the sample was redissolved in 0.7 mL CDCl3 for NMR spectroscopy. Approximately 2-4 mg of sample were dissolved in tetrahydrofuran (THF) for GPC.

Air-free photochemical reaction conditions – squalane

To a 1 dram vial with a septum cap, squalane (50 mg, 0.118 mmol, 1.00 equiv.) and photocatalyst (benzophenone, decatungstate, or ferric chloride) were dissolved in either DCM or 4:1 DCM:acetonitrile (2.3 mL total). A 0.7 cm stir bar was added and the vial was sealed. The solvent was purged with N_2 for 15 minutes. The vial was placed on a stir plate, 2 cm away from a Kessil 370 nm or 390 nm lamp and irradiated for 24 h. A fan was used to keep the temperature low. The solvent was removed, and the sample was redissolved in 0.7 mL $CDCl_3$ for NMR spectroscopy. Approximately 15 mg of ethylene carbonate (δ = 4.542 ppm) was added as an internal standard.

Photochemical reaction conditions in air – squalane

To a 1 dram vial with a septum cap, squalane (50 mg, 0.118 mmol, 1.00 equiv.) and photocatalyst (benzophenone, decatungstate, or ferric chloride) were dissolved in either DCM or 4:1 DCM:acetonitrile (2.3 mL total). A 0.7 cm stir bar was added and the vial was sealed. The septum was pierced with a needle, which was left in the septum for the duration

of the reaction. The vial was placed on a stir plate, 2 cm away from a Kessil 370 nm or 390 nm lamp and irradiated for 24 h. A fan was used to keep the temperature low. The solvent was removed, and the sample was redissolved in 0.7 mL $CDCl_3$ for NMR spectroscopy. Approximately 15 mg of ethylene carbonate (δ = 4.542 ppm) was added as an internal standard.

Synthesis of tetrabutylammonium decatungstate

To a 1 L beaker, tetrabutylammonium bromide (2.40 g, 7.45 mmol, 0.49 equiv.), deionized water (800 mL), and a 2" Teflon stir bar were added. To a separate 2 L beaker, sodium tungstate dihydrate (5.00 g, 15.15 mmol, 1.00 equiv.), deionized water (800 mL), and a 3" Teflon stir bar were added. Both beakers were wrapped with aluminum foil (for insulation) and heated to 90 °C with rapid stirring. When both solutions reached 90 °C, a small amount of concentrated HCl was added to both solutions until the pH stabilized at 2. The sodium tungstate dihydrate solution turned pale yellow green. The contents of the 1 L beaker were added to the 2 L beaker and a white precipitate formed. The contents of the beaker were stirred for an additional 30 minutes. The reaction was cooled to room temperature and filtered through a silica gel plug. The white powder was washed with water and dried under vacuum. The receiving flask was exchanged, and the silica plug was washed with acetonitrile (3 x 100 mL). The filtrate was collected, and the solvent was removed under vacuum. The filtrate was recrystallized from acetonitrile at -20 °C for 48 h. The crystals were washed with minimal cold acetonitrile and dried under vacuum. The recrystallization was performed again on the filtrate for a second crop of crystals (3.82 g, 1.151 mmol, 76% yield).

REFERENCES

(1) Williamson, J. B.; Lewis, S. E.; Johnson, R. R.; Manning, I. M.; Leibfarth, F. A. C−H Functionalization of Commodity Polymers. *Angew. Chem. Int. Ed.* **2019**, *58* (26), 8654–8668. https://doi.org/10.1002/anie.201810970.

(2) Rahimi, A.; García, J. M. Chemical Recycling of Waste Plastics for New Materials Production. *Nat. Rev. Chem.* **2017**, *1* (6), 1–11. https://doi.org/10.1038/s41570-017-0046.

(3) Singh, N.; Hui, D.; Singh, R.; Ahuja, I. P. S.; Feo, L.; Fraternali, F. Recycling of Plastic Solid Waste: A State of Art Review and Future Applications. *Compos. B. Eng.* **2017**, *115*, 409–422. https://doi.org/10.1016/j.compositesb.2016.09.013.

(4) *Plastics - the Facts 2021 • Plastics Europe*. Plastics Europe. https://plasticseurope.org/knowledge-hub/plastics-the-facts-2021/ (accessed 2022-09-22).

(5) Geyer, R.; Jambeck, J. R.; Law, K. L. Production, Use, and Fate of All Plastics Ever Made. *Sci. Adv.* **2017**, *3* (7), e1700782. https://doi.org/10.1126/sciadv.1700782.

(6) Jambeck, J. R.; Geyer, R.; Wilcox, C.; Siegler, T. R.; Perryman, M.; Andrady, A.; Narayan, R.; Law, K. L. Plastic Waste Inputs from Land into the Ocean. *Science* **2015**, *347* (6223), 768–771. https://doi.org/10.1126/science.1260352.

(7) Jehanno, C.; Alty, J. W.; Roosen, M.; De Meester, S.; Dove, A. P.; Chen, E. Y.-X.; Leibfarth, F. A.; Sardon, H. Critical Advances and Future Opportunities in Upcycling Commodity Polymers. *Nature* **2022**, *603* (7903), 803–814. https://doi.org/10.1038/s41586-021-04350-0.

(8) MacArthur, D. E.; Waughray, D.; Stuchtey, M. R. The New Plastics Economy: Rethinking the Future of Plastics, 2016. https://www3.weforum.org/docs/WEF_The_New_Plastics_Economy.pdf.

(9) Kosloski-Oh, S. C.; Wood, Z. A.; Manjarrez, Y.; Rios, J. P. de los; Fieser, M. E. Catalytic Methods for Chemical Recycling or Upcycling of Commercial Polymers. *Mater. Horiz.* **2021**, *8* (4), 1084–1129. https://doi.org/10.1039/D0MH01286F.

(10) Zhang, M.; Colby, R. H.; Milner, S. T.; Chung, T. C. M.; Huang, T.; deGroot, W. Synthesis and Characterization of Maleic Anhydride Grafted Polypropylene with a Well-Defined Molecular Structure. *Macromolecules* **2013**, *46* (11), 4313–4323. https://doi.org/10.1021/ma4006632.

(11) Hamielec, A. E.; Gloor, P. E.; Zhu, S. Kinetics of, Free Radical Modification of Polyolefins in Extruders - Chain Scission, Crosslinking and Grafting. *Can. J. Chem. Eng.* **1991**, *69* (3), 611–618. https://doi.org/10.1002/cjce.5450690302.

(12) Hinsken, H.; Moss, S.; Pauquet, J.-R.; Zweifel, H. Degradation of Polyolefins during Melt Processing. *J. Polym. Degrad. Stab.* **1991**, *34* (1), 279–293. https://doi.org/10.1016/0141-3910(91)90123-9.

(13) Dainton, F. S.; Ivin, K. J. Reversibility of the Propagation Reaction in Polymerization Processes and Its Manifestation in the Phenomenon of a 'Ceiling Temperature'. *Nature* **1948**, *162* (4122), 705–707. https://doi.org/10.1038/162705a0.

(14) Allen, N. S.; Chirinos-Padron, A.; Henman, T. J. Photoinitiated Oxidation of Polypropylene: A Review. *Prog. Org. Coat.* **1985**, *13* (2), 97–122. https://doi.org/10.1016/0033-0655(85)80020-0.

(15) Abdouss, M.; Sharifi-Sanjani, N.; Bataille, P. Oxidation of Polypropylene in a Solution of Monochlorobenzene. *Journal of Applied Polymer Science* **1999**, *74* (14), 3417–3424. https://doi.org/10.1002/(SICI)1097-4628(19991227)74:14<3417::AID-APP16>3.0.CO;2-G.
(16) Sheel, A.; Pant, D. 6 - Chemical Depolymerization of Polyurethane Foams via Glycolysis and Hydrolysis. In *Recycling of Polyurethane Foams*; Thomas, S., Rane, A. V., Kanny, K., V.k., A., Thomas, M. G., Eds.; Plastics Design Library; William Andrew Publishing, 2018; pp 67–75. https://doi.org/10.1016/B978-0-323-51133-9.00006-1.
(17) Anuar Sharuddin, S. D.; Abnisa, F.; Wan Daud, W. M. A.; Aroua, M. K. A Review on Pyrolysis of Plastic Wastes. *J. En. Con. Man.* **2016**, *115*, 308–326. https://doi.org/10.1016/j.enconman.2016.02.037.
(18) Diaz-Silvarrey, L. S.; Zhang, K.; Phan, A. N. Monomer Recovery through Advanced Pyrolysis of Waste High Density Polyethylene (HDPE). *Green Chem.* **2018**, *20* (8), 1813–1823. https://doi.org/10.1039/C7GC03662K.
(19) Celik, G.; Kennedy, R. M.; Hackler, R. A.; Ferrandon, M.; Tennakoon, A.; Patnaik, S.; LaPointe, A. M.; Ammal, S. C.; Heyden, A.; Perras, F. A.; Pruski, M.; Scott, S. L.; Poeppelmeier, K. R.; Sadow, A. D.; Delferro, M. Upcycling Single-Use Polyethylene into High-Quality Liquid Products. *ACS Cent. Sci.* **2019**, *5* (11), 1795–1803. https://doi.org/10.1021/acscentsci.9b00722.
(20) Conk, R. J.; Hanna, S.; Shi, J. X.; Yang, J.; Ciccia, N. R.; Qi, L.; Bloomer, B. J.; Heuvel, S.; Wills, T.; Su, J.; Bell, A. T.; Hartwig, J. F. Catalytic Deconstruction of Waste Polyethylene with Ethylene to Form Propylene. *Science* **2022**, *377* (6614), 1561–1566. https://doi.org/10.1126/science.add1088.
(21) Arroyave, A.; Cui, S.; Lopez, J. C.; Kocen, A. L.; LaPointe, A. M.; Delferro, M.; Coates, G. W. Catalytic Chemical Recycling of Post-Consumer Polyethylene. *J. Am. Chem. Soc.* **2022**, *144* (51), 23280–23285. https://doi.org/10.1021/jacs.2c11949.
(22) Sarkar, S.; Cheung, K. P. S.; Gevorgyan, V. C–H Functionalization Reactions Enabled by Hydrogen Atom Transfer to Carbon-Centered Radicals. *Chem. Sci.* **2020**, *11* (48), 12974–12993. https://doi.org/10.1039/D0SC04881J.
(23) Capaldo, L.; Ravelli, D.; Fagnoni, M. Direct Photocatalyzed Hydrogen Atom Transfer (HAT) for Aliphatic C–H Bonds Elaboration. *Chem. Rev.* **2022**, *122* (2), 1875–1924. https://doi.org/10.1021/acs.chemrev.1c00263.
(24) Fazekas, T. J.; Alty, J. W.; Neidhart, E. K.; Miller, A. S.; Leibfarth, F. A.; Alexanian, E. J. Diversification of Aliphatic C–H Bonds in Small Molecules and Polyolefins through Radical Chain Transfer. *Science* **2022**, *375* (6580), 545–550. https://doi.org/10.1126/science.abh4308.
(25) Williamson, J. B.; Czaplyski, W. L.; Alexanian, E. J.; Leibfarth, F. A. Regioselective C−H Xanthylation as a Platform for Polyolefin Functionalization. *Angew. Chem. Int. Ed.* **2018**, *57* (21), 6261–6265. https://doi.org/10.1002/anie.201803020.
(26) Williamson, J. B.; Na, C. G.; Johnson, R. R.; Daniel, W. F. M.; Alexanian, E. J.; Leibfarth, F. A. Chemo- and Regioselective Functionalization of Isotactic Polypropylene: A Mechanistic and Structure–Property Study. *J. Am. Chem. Soc.* **2019**, *141* (32), 12815–12823. https://doi.org/10.1021/jacs.9b05799.

(27) Oh, S.; Stache, E. E. Chemical Upcycling of Commercial Polystyrene via Catalyst-Controlled Photooxidation. *J. Am. Chem. Soc.* **2022**, *144* (13). https://doi.org/10.1021/jacs.2c01411.
(28) Li, T.; Vijeta, A.; Casadevall, C.; Gentleman, A. S.; Euser, T.; Reisner, E. Bridging Plastic Recycling and Organic Catalysis: Photocatalytic Deconstruction of Polystyrene via a C–H Oxidation Pathway. *ACS Catal.* **2022**, *12* (14), 8155–8163. https://doi.org/10.1021/acscatal.2c02292.
(29) Kong, S.; He, C.; Dong, J.; Li, N.; Xu, C.; Pan, X. Sunlight-Mediated Degradation of Polyethylene under the Synergy of Photothermal C-H Activation and Modification. *Macromol. Chem. Phys.* **2022**, *223* (12), 2100322. https://doi.org/10.1002/macp.202100322.
(30) Bertin, D.; Leblanc, M.; Marque, S. R. A.; Siri, D. Polypropylene Degradation: Theoretical and Experimental Investigations. *Polymer Degradation and Stability* **2010**, *95* (5), 782–791. https://doi.org/10.1016/j.polymdegradstab.2010.02.006.
(31) Mita, I.; Obata, K.; Horie, K. Photoinitiated Thermal Degradation of Polymers II. Poly(Methyl Methacrylate). *Polym. J.* **1990**, *22* (5), 397–410. https://doi.org/10.1295/polymj.22.397.
(32) Yousif, E.; Haddad, R. Photodegradation and Photostabilization of Polymers, Especially Polystyrene: Review. *SpringerPlus* **2013**, *2* (1), 398. https://doi.org/10.1186/2193-1801-2-398.
(33) Tian, X.; Ding, J.; Zhang, B.; Qiu, F.; Zhuang, X.; Chen, Y. Recent Advances in RAFT Polymerization: Novel Initiation Mechanisms and Optoelectronic Applications. *Polymers (Basel)* **2018**, *10* (3), 318. https://doi.org/10.3390/polym10030318.
(34) Qu, B.; Xu, Y.; Ding, L.; Rånby, B. A New Mechanism of Benzophenone Photoreduction in Photoinitiated Crosslinking of Polyethylene and Its Model Compounds. *J. Polym. Sci. A Polym. Chem.* **2000**, *38* (6), 999–1005. https://doi.org/10.1002/(SICI)1099-0518(20000315)38:6<999::AID-POLA9>3.0.CO;2-1.
(35) Dondi, D.; Ravelli, D.; Fagnoni, M.; Mella, M.; Molinari, A.; Maldotti, A.; Albini, A. Regio- and Stereoselectivity in the Decatungstate Photocatalyzed Alkylation of Alkenes by Alkylcyclohexanes. *Chem. Eur. J.* **2009**, *15* (32), 7949–7957. https://doi.org/10.1002/chem.200900810.
(36) Laudadio, G.; Govaerts, S.; Wang, Y.; Ravelli, D.; Koolman, H. F.; Fagnoni, M.; Djuric, S. W.; Noël, T. Selective C(Sp3)−H Aerobic Oxidation Enabled by Decatungstate Photocatalysis in Flow. *Angew. Chem. Int. Ed.* **2018**, *57* (15), 4078–4082. https://doi.org/10.1002/anie.201800818.
(37) Luo, Y.-R. *Comprehensive Handbook of Chemical Bond Energies*, 1st ed.; CRC Press: 6000 Broken Sound Parkway, NW, Suite 300, Boca Raton, FL 33487-2742, 2007.
(38) Negishi, A.; Ogiwara, Y. ESR Study of the Effect of Ferric Chloride on the Photodegradation of Model Compound for Polypropylene. *J. Appl. Polym. Sci.* **1980**, *25* (6), 1095–1104. https://doi.org/10.1002/app.1980.070250612.
(39) Duncan, D. C.; Netzel, T. L.; Hill, C. L. Early-Time Dynamics and Reactivity of Polyoxometalate Excited States. Identification of a Short-Lived LMCT Excited State and a Reactive Long-Lived Charge-Transfer Intermediate Following Picosecond

Flash Excitation of [W10O32]4- in Acetonitrile. *Inorg. Chem.* **1995**, *34* (18), 4640–4646. https://doi.org/10.1021/ic00122a021.
(40) Renneke, R. F.; Pasquali, M.; Hill, C. L. Polyoxometalate Systems for the Catalytic Selective Production of Nonthermodynamic Alkenes from Alkanes. Nature of Excited-State Deactivation Processes and Control of Subsequent Thermal Processes in Polyoxometalate Photoredox Chemistry. *J. Am. Chem. Soc.* **1990**, *112* (18), 6585–6594. https://doi.org/10.1021/ja00174a020.
(41) Ravelli, D.; Fagnoni, M.; Fukuyama, T.; Nishikawa, T.; Ryu, I. Site-Selective C–H Functionalization by Decatungstate Anion Photocatalysis: Synergistic Control by Polar and Steric Effects Expands the Reaction Scope. *ACS Catal.* **2018**, *8* (1), 701–713. https://doi.org/10.1021/acscatal.7b03354.
(42) Perry, I. B.; Brewer, T. F.; Sarver, P. J.; Schultz, D. M.; DiRocco, D. A.; MacMillan, D. W. C. Direct Arylation of Strong Aliphatic C–H Bonds. *Nature* **2018**, *560* (7716), 70–75. https://doi.org/10.1038/s41586-018-0366-x.
(43) Yamase, T.; Takabayashi, N.; Kaji, M. Solution Photochemistry of Tetrakis(Tetrabutylammonium) Decatungstate(VI) and Catalytic Hydrogen Evolution from Alcohols. *J. Chem. Soc., Dalton Trans.* **1984**, No. 5, 793–799. https://doi.org/10.1039/DT9840000793.
(44) Protti, S.; Ravelli, D.; Fagnoni, M.; Albini, A. Solar Light-Driven Photocatalyzed Alkylations. Chemistry on the Window Ledge. *Chem. Commun.* **2009**, No. 47, 7351–7353. https://doi.org/10.1039/B917732A.
(45) Ravelli, D.; Protti, S.; Fagnoni, M. Decatungstate Anion for Photocatalyzed "Window Ledge" Reactions. *Acc. Chem. Res.* **2016**, *49* (10), 2232–2242. https://doi.org/10.1021/acs.accounts.6b00339.
(46) Ryu, I.; Tani, A.; Fukuyama, T.; Ravelli, D.; Montanaro, S.; Fagnoni, M. Efficient C–H/C–N and C–H/C–CO–N Conversion via Decatungstate-Photoinduced Alkylation of Diisopropyl Azodicarboxylate. *Org. Lett.* **2013**, *15* (10), 2554–2557. https://doi.org/10.1021/ol401061v.
(47) Waele, V. D.; Poizat, O.; Fagnoni, M.; Bagno, A.; Ravelli, D. Unraveling the Key Features of the Reactive State of Decatungstate Anion in Hydrogen Atom Transfer (HAT) Photocatalysis. *ACS Catal.* **2016**, *6* (10), 7174–7182. https://doi.org/10.1021/acscatal.6b01984.
(48) Keer, L. D.; Steenberge, P. V.; Reyniers, M.-F.; Gryn'ova, G.; Aitken, H. M.; Coote, M. L. New Mechanism for Autoxidation of Polyolefins: Kinetic Monte Carlo Modelling of the Role of Short-Chain Branches, Molecular Oxygen and Unsaturated Moieties. *Polym. Chem.* **2022**, *13* (22), 3304–3314. https://doi.org/10.1039/D1PY01659H.
(49) Garrett, G. E.; Pratt, D. A.; Parent, J. S. Hydrogen Atom Abstraction from Polyolefins: Experimental and Computational Studies of Model Systems. *Macromolecules* **2020**, *53* (8), 2793–2800. https://doi.org/10.1021/acs.macromol.9b02091.
(50) Taylor, L. J.; Tobias, J. W. Accelerated Photo-Oxidation of Polyethylene. II. Further Evaluation of Selected Additives. *J. Appl. Polym. Sci.* **1981**, *26* (9), 2917–2926. https://doi.org/10.1002/app.1981.070260908.

(51) Juliá, F. Ligand-to-Metal Charge Transfer (LMCT) Photochemistry at 3d-Metal Complexes: An Emerging Tool for Sustainable Organic Synthesis. *ChemCatChem* **2022**, *14* (19), e202200916. https://doi.org/10.1002/cctc.202200916.
(52) Zhang, G.; Zhang, Z.; Zeng, R. Photoinduced FeCl3-Catalyzed Alkyl Aromatics Oxidation toward Degradation of Polystyrene at Room Temperature†. *Chin. J. Chem.* **2021**, *39* (12), 3225–3230. https://doi.org/10.1002/cjoc.202100420.
(53) Huang, Z.; Shanmugam, M.; Liu, Z.; Brookfield, A.; Bennett, E. L.; Guan, R.; Vega Herrera, D. E.; Lopez-Sanchez, J. A.; Slater, A. G.; McInnes, E. J. L.; Qi, X.; Xiao, J. Chemical Recycling of Polystyrene to Valuable Chemicals via Selective Acid-Catalyzed Aerobic Oxidation under Visible Light. *J. Am. Chem. Soc.* **2022**, *144* (14), 6532–6542. https://doi.org/10.1021/jacs.2c01410.
(54) Klein, D. *Organic Chemistry*, 2nd ed.; John Wiley & Sons, Ltd, 2015.